INSTITUTE OF PLASMA PHYSICS

NAGOYA UNIVERSITY

RESEARCH REPORT

NAGOYA, JAPAN

Damping Of Radial Oscillation Of A Toroidal Pinch Plasma

Mikio Mimura

IPPJ-305 September 1977

Further communication about this report is to be sent to the Research Information Center, Institute of Plasma Physics, Nagoya University, Nagoya, Japan.

ABSTRACT

Damping of radial oscillation which is observed in the early phase of pinch discharges is studied in a toroidal pinch machine, STP-2. Since the experiment is carried out in the toroidal machine, it becomes possible to ignore the endloss effect which cannot be avoided in linear machines. The temporal evolution of the oscillation is measured with a diamagnetic loop, and the plasma temperature and density are obtained by laser scattering. The temperature varies from 5 to 30 eV, and the density from 2×10^{15} to $1 \times 10^{16}/cm^3$. The temperature dependence of the observed damping time is compared with the result calculated from MHD equations which include dissipation terms. It is shown that the oscillation damps due to resistivity at low temperature while ion viscous damping is dominant at high temperature.

1. INTRODUCTION

Recently it was suggested that the damping of radial oscillation of pinch plasma will be useful for further heating of high beta plasma.[1] The radial oscillation of pinch plasma has been well known for a long time.[2] It was identified to be a magneto-acoustic oscillation of m = 0 mode, which is excited by the compression of plasma at the implosion phase of the discharge. Here, m is the wave number in poloidal direction. In 1959, Niblett and Green explained this oscillation using a simple model which consists of bias field inside of an annulus plasma layer and magnetic field outside of it.[3] They showed that the period of the oscillation is expressed as:

$$\tau = 2\pi \left(\frac{N m_i}{H^2} \right)^{\frac{1}{2}}$$

Here, H is the magnetic field, N is the line density of the plasma, and m_i is the ion mass in the plasma. This relation was often used to estimate the line density of pinch plasmas. Damping of the oscillation, however, has not been studied much. The main reason for it is that the experimental study on the oscillation in the past were done mainly in linear machines. In such machines, the endloss of the plasma has a strong influence on the damping of the oscillation and the study on the physical mechanism of the damping process becomes difficult. Therefore the experiment should be carried out in toroidal machines. Although the radial oscillation were observed in several toroidal machines,[4,5] sufficient data for the study of the damping process were not obtained. In

this paper, damping of the radial oscillation which appears in the early phase of a toroidal pinch discharge is studied experimentally. In order to clarify its physical mechanism, the experimental results are compared with the calculated results from MHD equations which include dissipation terms.

2. EXPERIMENTAL SETUP

The experiments are carried out in STP (Symmetrical Toroidal Pinch)-2 machine.[6,7] A schematic drawing of STP-2 and the diagnostics are shown in Fig.1. The discharge tube is made of quartz torus with the major radius of 25 cm and the minor radius of 10 cm. Double copper shell structure is adopted to reduce the stray field near the tub of the induction coil. Inner shell is used as the conducting shell to get the equilibrium of the plasma column, and the outer shell is used as the induction coil to induce the current in the plasma. Outside of the shells are set the toroidal field coils.

The radial oscillation is observed by measuring the toroidal flux change with a so-called diamagnetic loop.[8] The vacuum field component in the signal of the diamagnetic loop is cancelled by the signal of the Rogowskii coil which measures the toroidal coil current. The toroidal field distribution in the plasma is measured with magnetic probes inserted into the plasma. The electron temperature and density are obtained by laser scattering. The laser used here is a Ruby laser with the energy of 1.2 J. A monocromator, NIKON P-250 (30 Å/mm dispersion) is used with the slit width of 0.6 mm.

The motion of the plasma column in major radius direction is monitored with a streak camera.

Figure 2 shows the sequence of the discharge, and typical wave forms of toroidal field B_z and plasma current I_p. Deuterium gas is introduced into the discharge tube through a fast acting gas valve. The initial gas pressure in the tube is varied from 5×10^{-3} Torr to 4×10^{-2} Torr. Pre-ionization is made by an RF field of 3 MHz applied at the glass port. When the gas in the tube becomes homogeneous, the bias field is applied. When it reaches to 330 G, the toroidal current of 8 kA is induced for preheating. After 19 μsec, the main discharges are applied. The toroidal field rises to its maximum value of 9.4 kG in 5.5 μsec. At the peak it is crowbared, then it decreases with the decay time of about 90 μsec. The plasma current rises to 74 kA in 4.6 μsec and decreases with the decay time of about 55 μsec.

3. EXPERIMENTAL RESULTS

The radial oscillation of the plasma column is seen in the streak pictures, in the diamagnetic loop signal, and in the signals of the magnetic probes. Figure 3 shows typical examples of the signals in a case of the filling pressure of 2×10^{-2} Torr. As is shown in Fig.1, the diamagnetic loop and the magnetic probes are positioned to make an angle of 120° in toroidal direction. The phases of the oscillation of these two signals are seen to coincide. This means that the mode of the observed oscillation is $k = 0$. Here, k is

the wave number in toroidal direction, Figure 4 shows the internal toroidal field distributions at the first compression (a), and at the first expansion (b). They are normalized by the vacuum field at each position. At the compression phase, the distribution becomes paramagnetic-like, because the field in the plasma is compressed. At the expansion phase, it becomes diamagnetic-like. It is apparently seen that the oscillation is in the fundamental mode in the small radial direction.

Figure 5 shows the signals from the diamagnetic loop with the filling pressure as a parameter. It is seen that the amplitude and the period increase as the filling pressure. Figure 6 shows the period of the oscillation versus the filling pressure. Since the magnetic field is increasing with time, its values at three different moments are plotted to examine the dependence on the magnetic field. As will be derived in the next section, the period calculated from MHD equations is written as the following form in the present plasma parameters:

$$\tau = 1.25\sqrt{P_o}/B_z \qquad (1)$$

Here, the period τ is expressed in μsec, the initial filling pressure P_o in 10^{-3} Torr and the toroidal field B_z in kG. Three curves for calculated period which correspond to the experimental data are plotted in Fig.6. Agreement between the observed period and calculated one is quite good.

Now we study the temporal evolution of the flux change $\Delta\Phi$. Because the total flux Φ is increasing with time, it is appropriate to introduce the normalized flux change $\Delta\Phi/\Phi$.

In the present experimental parameters, it is expressed as:

$$\Delta\Phi/\Phi \propto \frac{\Delta\Phi}{\sin \frac{90^\circ}{5.5\times10^{-6}}t}$$

Figure 7 shows its temporal evolution for five different filling pressure. The curves are seen to be classified into two groups; concave-like curves (a, b, c) and S-like curves (d, e). The first curves (a, b, c) belong to the condition of the filling pressure higher than 2×10^{-2} Torr. The damping time of them increases monotonically with time. The second curves (d, e) are in the case of the lower filling pressure. The damping time of them increases at first, then decreases. Figure 8 shows the average damping time of $\Delta\Phi/\Phi$ over the time interval between 3.5 μsec and 4.5 μsec as a function of the filling pressure. The typical feature of the damping time is that it is not a monotone function of the filling pressure. It increases with the pressure till it reaches to the maximum at the pressure of 2×10^{-2} Torr. It decreases with the pressure when the pressure is higher than 2×10^{-2} Torr.

The electron temperature and density measured by laser scattering are plotted versus the filling pressure in Fig.9. They were measured at the center of the plasma column at 4 μsec from the start of the main discharge. When the filling pressure is varied from 5×10^{-3} Torr to 4×10^{-2} Torr, the temperature varies from 30 to 4 eV while the density changes from 2×10^{15} to $1 \times 10^{16}/cm^3$.

4. THEORETICAL CONSIDERATION

Discussions on the m = 0, k = 0 radial oscillation have already been made theoretically in the past without taking the dissipative effects into consideration. Although the period of the oscillation is derived in such a case, its damping cannot be discussed. Braginskii treated the damping of magneto-acoustic waves from the viewpoint of entropy production.[9] However, his analysis was limited to one dimensional geometry. In this section, damping of the oscillation of cylindrical plasma is derived directly by solving the MHD equations which include dissipation terms. As is estimated in Appendix, thermal conduction, particle diffusion, and energy loss due to netural particles have small influences on the damping of the oscillation. The main dissipation terms are considered to be plasma resistivity and viscosity terms.

The motion of the plasma is described by the following basic equations:

$$\rho \frac{d\mathbf{v}}{dt} = -\nabla p + \mathbf{j} \times \mathbf{B} - \frac{\partial \Pi}{\partial x} , \qquad (2)$$

$$\frac{\partial \rho}{\partial t} + \nabla(\rho \mathbf{v}) = 0 , \qquad (3)$$

$$\mathbf{E} + \mathbf{v} \times \mathbf{B} = \frac{\mathbf{j}}{\sigma} , \qquad (4)$$

$$\nabla \times \mathbf{B} = \mu_0 \mathbf{j} , \qquad (5)$$

$$\nabla \cdot \mathbf{B} = 0 , \qquad (6)$$

$$\nabla \times \mathbf{E} = -\frac{\partial \mathbf{B}}{\partial t} , \qquad (7)$$

$$\frac{1}{p}\frac{dp}{dt} = \frac{\gamma}{\rho}\frac{d\rho}{dt} , \qquad (8)$$

where Π is the stress tensor, σ is the conductivity of the plasma, and for other quantities, the usual notations are used.

We solve above equations following the procedure used to solve the MHD equations which do not include dissipation terms.[10] A simplified model shown in Fig.10 is adopted. Plasma is an infinitely long cylinder of radius a, surrounded by vacuum, bounded at r = b by a conducting shell. The current flows only on the surface of the plasma, so that the magnetic field inside the plasma has only the z-component B_z. The radial oscillation is treated as a small deviation from the equilibrium state. The unperturbed density and pressure of the plasma are ρ_o and p_o, respectively. Since we are interested in the m = 0, k = 0 mode only,

$$\frac{\partial}{\partial \theta} = \frac{\partial}{\partial z} = 0 \quad .$$

Then it is shown that the perturbed velocity v_1 and magnetic field B_1 in the plasma have only the r-component and the z-component, respectively. We develop the quantities into orders ($\rho = \rho_o + \rho_1$, $v = v_o + v_1$, $B = B_z + B_1$, etc.). In cylindrical coordinates, the equations for the first order quantities becomes as follows, where $\eta_{//}$ and $\eta_\perp$ are the parallel and perpendicular viscosity coefficients, respectively.

$$\frac{\partial \rho_1}{\partial t} + \frac{1}{r}\frac{\partial}{\partial r}(r \rho_0 v_1) = 0 \quad , \tag{9}$$

$$\rho_0 \frac{\partial v_1}{\partial t} = -\frac{\partial p_1}{\partial r} - \frac{1}{\mu_0} B_z \frac{\partial B_1}{\partial r} + \left(\frac{\eta_{//}}{3} + \eta_\perp\right)\frac{\partial}{\partial r}\frac{1}{r}\frac{\partial}{\partial r}(r v_1) \quad , \tag{10}$$

$$\frac{\partial B_1}{\partial t} + B_z \frac{1}{r}\frac{\partial}{\partial r}(r v_1) + \frac{1}{\mu_0 \sigma}\frac{1}{r}\frac{\partial}{\partial r} r \frac{\partial B_1}{\partial r} = 0 \quad , \tag{11}$$

$$\frac{\partial p_1}{\partial t} = -\frac{\gamma p_0}{r}\frac{\partial}{\partial r}(r v_1) \quad . \tag{12}$$

Elimination of ρ_1 and p_1 yields coupled differential equations for v_1 and B_1.

$$\rho_0 \frac{\partial^2 v_1}{\partial t^2} = \gamma p_0 \frac{\partial}{\partial r}\left(\frac{1}{r}\frac{\partial}{\partial r}(r v_1)\right) - \frac{B_z}{\mu_0}\frac{\partial}{\partial t}\frac{\partial B_1}{\partial r} + \left(\frac{\eta_\parallel}{3}+\eta_\perp\right)\frac{\partial}{\partial t}\frac{\partial}{\partial r}\frac{1}{r}\frac{\partial}{\partial r}(r v_1), \quad (13)$$

$$\frac{\partial B_1}{\partial t} + B_z \frac{1}{r}\frac{\partial}{\partial r}(r v_1) + \frac{1}{\mu_0 \sigma}\frac{1}{r}\frac{\partial}{\partial r} r \frac{\partial B_1}{\partial r} = 0 . \quad (14)$$

In the case when the dissipation terms are ignored ($\sigma = \infty$, $\eta_\parallel = \eta_\perp = 0$), these equations have the following solutions:[10]

$$v_1 = C\,(V_A^2 + V_s^2)^{\frac{1}{2}}\, J_1(k_0 r)\, e^{-i\omega_0 t}, \quad (15)$$

$$B_1 = i\, C\, B_z\, J_0(k_0 r)\, e^{-i\omega_0 t}, \quad (16)$$

where C is a dimensionless constant, $V_A^2 = B_z^2/\mu_0\rho_0$ (Alfvén velocity), $V_s^2 = \gamma p_0/\rho_0$ (sound velocity), and J_0, J_1 are Bessel functions of zeroth order and first order, respectively. The frequency ω_0 and the wave number in the radial direction k_0 are obtained by solving Maxwell's equations in the vacuum region and applying the boundary condition at the plasma surface. The results are:

$$\omega_0 = k_0\,(V_A^2 + V_s^2)^{\frac{1}{2}}, \quad (17)$$

$$k_0 = \frac{V_{A\theta}^2\,(1 - k_0^{-1} b/a) - V_{A0}^2\,\frac{2a^2}{b^2-a^2}}{a}\,\frac{J_1(k_0 a)}{J_0(k_0 a)}, \quad (18)$$

where $V_{A\theta}^2 = B_\theta^2/\mu_0\rho_0$ and $V_{A0}^2 = B_v^2/\mu_0\rho_0$.

The equation (1) in the previous section is derived from the above two equations by the following procedure.

Substituting the plasma parameters of STP-2 into the equation (18), we find the value of $k_o a$ to be about 2.7. Substituting ρ_o ($= n_o m b^2/a^2$) calculated from the filling pressure and adopting that $V_s \ll V_A$, we obtain the equation (1).

Now we introduce the dissipative effects to study the damping of the oscillation. It is reasonable to assume the dissipation terms as small perturbations. The frequency ω_o is modified by these diffipation terms. The equations (15), (16) are used as the unperturbed solutions of (13), (14). We assume the solutions as in the following forms:

$$v_1 = C (V_A^2 + V_s^2)^{\frac{1}{2}} J_1(k_0 r) e^{-i\omega t}, \qquad (19)$$

$$B_1 = i C B_z J_0(k_0 r) e^{-i\omega t}, \qquad (20)$$

which are to be substituted in (13), (14). Applying first the property of the Bessel functions, we get:

$$\frac{1}{r}\frac{\partial}{\partial r} r \frac{\partial B_1}{\partial r} = -k_0^2 B_1 .$$

From (14), we obtain:

$$B_1 = \left(\frac{1}{i\omega} + \frac{k_0^2}{\omega^2 \sigma \mu_0}\right) B_z \frac{1}{r}\frac{\partial}{\partial r}(r v_1). \qquad (21)$$

Substituting this relation into (13), we find:

$$-\omega^2 v_1 = \left(\frac{\gamma P_0}{\rho_0} + \frac{B_z^2}{\rho_0 \mu_0} - \frac{i k_0^2 B_z^2}{\omega \sigma \mu_0^2 \rho_0} - \frac{i\omega}{\rho_0}\left(\frac{\eta_\parallel}{3} + \eta_\perp\right)\right)\frac{\partial}{\partial r}\left(\frac{1}{r}\frac{\partial}{\partial r}(r v_1)\right)$$

$$= -k_0^2 \left(V_A^2 + V_s^2 - \frac{i k_0^2 B_z^2}{\omega \sigma \mu_0^2 \rho_0} - \frac{i\omega}{\rho_0}\left(\frac{\eta_\parallel}{3} + \eta_\perp\right)\right) v_1 .$$

As the dissipation terms are small, it reduces to

$$\omega = \omega_0 - \frac{i k_0^2}{2\sigma\mu_0} \frac{V_A^2}{V_A^2 + V_s^2} - i \frac{\left(\frac{\eta_{11}}{3} + \eta_\perp\right)}{2\rho_0} k_0^2 . \qquad (22)$$

The imaginary part appears due to the included dissipation terms. Thus the damping of the oscillation is described by:

$$e^{-i\omega t} = e^{-i\omega_0 t - \frac{t}{\tau_r} - \frac{t}{\tau_v}} . \qquad (23)$$

Here, τ_r and τ_v, the damping time due to resistivity and viscosity, respectively are:

$$\tau_r = \frac{2\sigma\mu_0}{k_0^2} \frac{V_A^2 + V_s^2}{V_A^2} , \qquad (24)$$

$$\tau_v = \frac{2\rho_0}{\left(\frac{\eta_{11}}{3} + \eta_\perp\right) k_0^2} . \qquad (25)$$

These expressions are found to agree with those derived by Braginskii except the interpretation of k_0.

5. DISCUSSIONS

In the chapter 3, the value of $k_0 a$ was derived to be 2.7, and the period of the oscillation calculated from (17) was found to agree well with the experimental results. Now we calculate the values of the damping time from (24) and (25) to compare with the result of the experiment. Using the plasma parameters of STP-2, we get:

$$\tau_r = 3.3 \times 10^{-2} T_e^{\frac{3}{2}} a^2 , \qquad (26)$$

$$\tau_v = 9.33 \times 10^{-25} \frac{na^2}{\left(\frac{\eta_{//}}{3} + \eta_\perp\right)} , \qquad (27)$$

where the following relations[9] are used.

$$\sigma = 0.9 \times 10^{13} T_e^{\frac{3}{2}} ,$$

$$\eta_{//} = 4.53 \times 10^{-6} T_i^{\frac{5}{2}} ,$$

$$\eta_\perp = \eta_{//} (5x^2 + 2.32) / (16x^4 + 16.12x^2 + 2.33) ,$$

$$x = \omega_i \tau_i .$$

Here, ω_i is the ion gyrofrequency and τ_i is the ion-ion collision time. The temperature is expressed in eV, σ in sec^{-1}, and other quantities in cgs. The perpendicular viscosity $\eta_\perp$ has the same order of magnitude as $\eta_{//}$ when the temperature is below 10 eV. It becomes negligibly small at the temperature higher than 20 eV. As is seen from (26) and (27), τ_r increases rapidly with the temperature, while τ_v has a dependence of $T_i^{5/2}$. Because both of them are proportional to the square of the plasma radius, we use the normalized damping time τ_d/a^2 to compare with the experimental results. Here,

$$\frac{1}{\tau_d} = \frac{1}{\tau_r} + \frac{1}{\tau_v} .$$

In Fig. 11 we plot τ_d/a^2 as a function of the electron temperature. We assumed that $T_i = T_e$, and used the relation between the density and the temperature obtained from laser scattering (Fig.9):

$$n_e = 2.3 \times 10^{16} T_e^{-\frac{2}{3}} .$$

As for B_z, the value at 4 μsec (8 kG) is employed. As is seen,

a maximum value appeares when the temperature is 12 eV. In the lower temperature side, the damping is mainly due to the resistivity, and in the higher temperature side, it is controlled by the viscosity.

The experimental values of τ_d/a^2 are also plotted on the same figure. In these data, plasma radius is deduced from the streak pictures. The fitting of the experimental values to the calculated curve is fairly good. Thus it can be concluded that the oscillation observed in the experiment is damped by the resistivty at low twmperature, and by the viscosity at high temperature. This conclusion also explains the temporal evolution of $\Delta\Phi/\Phi$ in Fig.7. Because the temperature increases during the implosion phase, the damping time is also a function of time. When the filling pressure is higher than 2×10^{-2} Torr, the temperature does not reach to 12 eV, so that the damping time increases monotonically with time. Therefore the curves of $\Delta\Phi/\Phi$ become concave-like(a, b, c). When the filling pressure is lower than 2×10^{-2} Torr, the temperature exceeds 12 eV. The damping time turns down due to the overwhelming viscous damping at that moment. Consequently the curves becomes S-like(d, e).

From the above concideration, it is reasonable to expect the damping of the oscillation for the further heating of the high-β plasma. The efficiency of Joule heating decreases as the temperature increases. On the contrary, the efficiency of the heating which uses the viscous damping increases as $T_i^{\frac{5}{2}}$ as long as the MHD model is applicable. For STP-2 plasma, it is roughly estimated that the MHD model is applicable when the

temperature is lower than 50 eV. In the higher temperature region than that, another approach which uses the kinetic model is needed.

6. SUMMARY

The physical mechanism of the damping of the m = 0, k = 0 radial oscillation is studied experimentally in a toroidal pinch machine STP-2. The period of the observed oscillation agrees quite well with that calculated from the ideal MHD equations. The damping time of the oscillation varies from 1 μsec to 4 μsec depending on the filling pressure. It takes the maximum value when the pressure is 2×10^{-2} Torr.

In order to explain the experimental results, MHD equations which include the dissipation terms are solved in the cylindrical geometry. Damping time due to the resistivity is derived to be $\tau_r = \frac{2\sigma\mu_o}{k_o^2} \frac{V_A^2 + V_S^2}{V_A^2}$, which increases rapidly with the temperature. Damping time due to the viscosity is found to be $\tau_V = 2\rho_o/(\frac{\eta_{//}}{3} + \eta_\perp)k_o^2$, which has a dependence of $T_i^{-5/2}$. Total damping time takes the maximum value when the temperature is 12 eV.

The damping time observed in the experiment agrees fairly well with the calculated one in the temperature dependence and in the order of the magnitude. It is concluded that the damping of the oscillation is mainly due to the resistivity at low temperature, while is governed by the viscosity at high temperature. This conclusion suggests that the viscous damping of the MHD oscillation can be expected for the further heating of the high-β plasma.

ACKNOWLEDGEMENTS

The author would like to express sincere gratitude to Professor K. Hirano for his guidance during the course of this work. He is also indebted to Drs. S. Kitagawa, K. Sato, and M. Wakatani for their useful advice and helpful discussion. He also appreciates Professors T. Taniuchi, K. Miyamoto, and Y. Terashima for the helpful discussions. He acknowledges Mr. S. Yamaguchi for his laser scattering measurement, and Mr. T. Naito for the technical assistance. He is grateful to Professors K. Takayama and H. Yoshimura for their continuous encouragement.

APPENDIX Estimation of the effects of particle diffusion, heat conduction, and neutral particles on the damping of the oscillation.

(i) Particle diffusion

As is well known, the decay time of the density distribution due to particle diffusion is given by $\tau = a^2/(5.8D)$ when the distribution takes the form of $J_o(k_o r)$. Here the classical diffusion coefficient D is given by:[9]

$$D = \frac{m_e T_e}{e^2 B^2} \nu_{ei} .$$

We estimate the decay time of the density distribution of the oscillation due to this process. Substituting typical parameters of STP-2 plasma (B = 6 kG, n = $5 \times 10^{15}/cm^3$, T_e = 10 eV), we get

$$D \sim 1.6 \times 10^4 \ cm^2/sec .$$

Then the decay time becomes:

$$\tau = \frac{a^2}{5.8 D} = 10^{-4} = 100 \mu sec .$$

This value is sufficiently large compared to the period of the oscillation. Therefore the particle diffusion seems to have no influence on the damping of the oscillation.

(ii) Heat conduction

Decay time of the temperature distribution of $J_o(k_o r)$ due to heat conduction is given by

$$\tau_h = \frac{a^2 n}{5.8 K_\perp} .$$

The thermal conductivities are:

$$K_\perp^e = 4.66 \frac{n_e T_e \tau_e}{m_e (\omega_e \tau_e)^2}, \qquad \text{(for electron)}$$

$$K_\perp^i = 2 \frac{n_i T_i \tau_i}{m_i (\omega_i \tau_i)^2}, \qquad \text{(for ion)}$$

where temperature is expressed in eV, other quantities in cgs. For deuterium plasma, the cyclotron frequencies and the collision times are:

$$\omega_e = 1.76 \times 10^7 B, \quad \tau_e = 3.5 \times 10^4 T_e^{\frac{3}{2}} / n, \text{ (for electron)}$$

$$\omega_i = 0.48 \times 10^4 B, \quad \tau_i = 3 \times 10^6 T_i^{\frac{3}{2}} / n \text{ . (for ion)}$$

Therefore the thermal conductivities of STP-2 plasma are:

$$K_\perp^e = 1.03 \times 10^{32}, \quad K_\perp^i = 1.9 \times 10^{33}.$$

Then the decay time becomes:

$$\tau = 2.5 \times 10^{-6} = 2.5 \mu\text{sec}.$$

This value is three to five times as large as the period of the oscillation.

(iii) Neutral particles

It is difficult to evaluate directly the effect of neutral particles on the damping of the oscillation. Here, we estimate the energy loss of plasma due to the existence of the neutral particles. The dominant processes which occur between neutral and charged particles in plasma, and

their cross section near the energy of 10 eV are as follows:[11,12] (1) elastic scattering between electrons and neutral particles, $\sigma \sim 5 \times 10^{-18}$ cm^2, (2) elastic scattering between ions and neutral particles $\sigma \sim 2 \times 10^{-15}$ cm^2, (3) ionization of neutral particles by electrons, $\sigma \sim 0$, (4) ionization of neutral particles by ions, $\sigma \sim 0$, (5) charge exchange between ions and neutral particles, $\sigma \sim 5 \times 10^{-15}$ cm^2. Since ion and neutral particle have the same mass, elastic collision and charge exchange between them have the same effect for energy transfer. The total cross section for both collisions is about 7×10^{-15} cm^2, so that the collision frequency becomes $\nu = n\langle\sigma v\rangle \sim 1 \times 10^8$/sec. Therefore the thermal equilibrium between neutral particles and ions is achieved in much shorter time than the period of the oscillation. Because the neutral particles are not trapped by the magnetic field, they can move freely in the distance of mean free path δ. Consequently half of the neutral particles in the layer of thickness δ on the surface of the plasma can escape from the plasma. We evaluate the energy loss due to these escaping particles. Plasma energy per unit length is:

$$\pi a^2 (nkT \times 2) .$$

When the density of neutral particles is n_n, the energy carried out by them from plasma per collision time τ_c is:

$$2\pi a \delta \left(\frac{n_n}{2} kT\right) .$$

Its ratio to the total energy is:

$$\alpha = \frac{1}{2} \frac{\delta}{a} \frac{n_n}{n}$$

Assuming that a = 3 cm and T_i = 10 eV, we get $\delta = \nu/\nu = 10^{-2}$ cm. If neutral particles of 5 % exist in the plasma, the ratio becomes $\alpha = 8 \times 10^{-5}$. Because the temporal change of energy is $E = E_o e^{-\alpha t/\tau_c}$ the e-folding decay time of energy becomes 130 μsec. This value is long enough compared to the life time of the oscillation. Therefore the effect of neutral particles on the energy loss is neglected.

REFERENCES

(1) J. Choe, W. Grossmann, and C.E. Seyler; Bull. Am. Phys. Soc., (1976) 5E-2

(2) S.W. Cousins and A.A. Ware; Proc. Phys. Soc., B 64 (1951) 159

(3) G.B.F. Niblett and T.S. Green; Proc. Phys. Soc. 74 (1959) 737

(4) C. Bobeldijk, R.J.J. van Heijningen, J.A. Hoekzema, W. Kooyman, P.C.T. van der Laan, D.J. Maris, D. Oepts, and A.A.M. Oomens; Proc. 5th Int.Conf. on Plasma Phys. and Contr. Nucl. Fusion Res., Tokyo (1974) IAEA E9-1

(5) Y. Hirano, S. Kiyama, T. Shimada, and K. Ogawa; Bulletin of the Electrotechnical Laboratory 38 (1974) 151

(6) K. Hirano, S. Kitagawa, and M. Mimura; Phys. Rev. Lett. 32 (1974) 1104

(7) K. Hirano, S. Kitagawa, M. Mimura, Y. Kita, M. Ohi, T. Amano, and M. Wakatani; Proc. 5th Int. Conf. on Plasma Phys. and Contr. Nucl. Fusion Res., Tokyo (1974) IAEA E9-5

(8) K.A. Razumova; Plasma Physics 8 (1966) 791

(9) S.I. Braginskii; Review of Plasma Physics (ed., M.A. Leontovich, Consultant Bureau, New York, London, 1966) Vol.1

(10) W. Schuurman; Rijnhuizen Report 68-48 (1968)

(11) K. Takayanagi and H. Suzuki; Atomic Process Cross Section Data Vol.1 IPPJ-DT-48 (1975)

(12) S.C. Brown; Basic Data of Plasma Physics (The M.I.T. Press, Cambridge, Massachusetts, 1959)

FIGURE CAPTIONS

Fig.1. Schematic drawing of STP-2 and layout of the diagnostics.

Fig.2. Sequence of the discharge and typical wave forms of toroidal field B_z and plasma current I_p.

Fig.3. Typical examples of signals. (A) streak picture. (B) Diamagnetic loop. (C) Internal magnetic probe positioned at R = 26 cm.

Fig.4. Internal distribution of toroidal magnetic field B_z.

Fig.5. Signals from the diamagnetic loop with the filling pressure as a parameter.

Fig.6. Period of the radial oscillation. Symbols show the experimental data. Curves show the value calculated from the MHD theory. A: B_z = 5.6 kG, B: 6.5 kG, C: 7.9 kG.

Fig.7. Temporal evolution of $\Delta\Phi/\Phi$. a: $p_o = 4 \times 10^{-2}$ Torr, b: 3×10^{-2} Torr, c: 2×10^{-2} Torr, d: 1×10^{-2} Torr, e: 5×10^{-3} Torr.

Fig.8. Average damping time of $\Delta\Phi/\Phi$ as a function of the filling pressure.

Fig.9. Pressure dependence of the electron temperature and density.

Fig.10. Plasma model used for theoretical consideration.

Fig.11. Normalized damping time. Curve shows the theoretical value. Open circles show the experimental data.

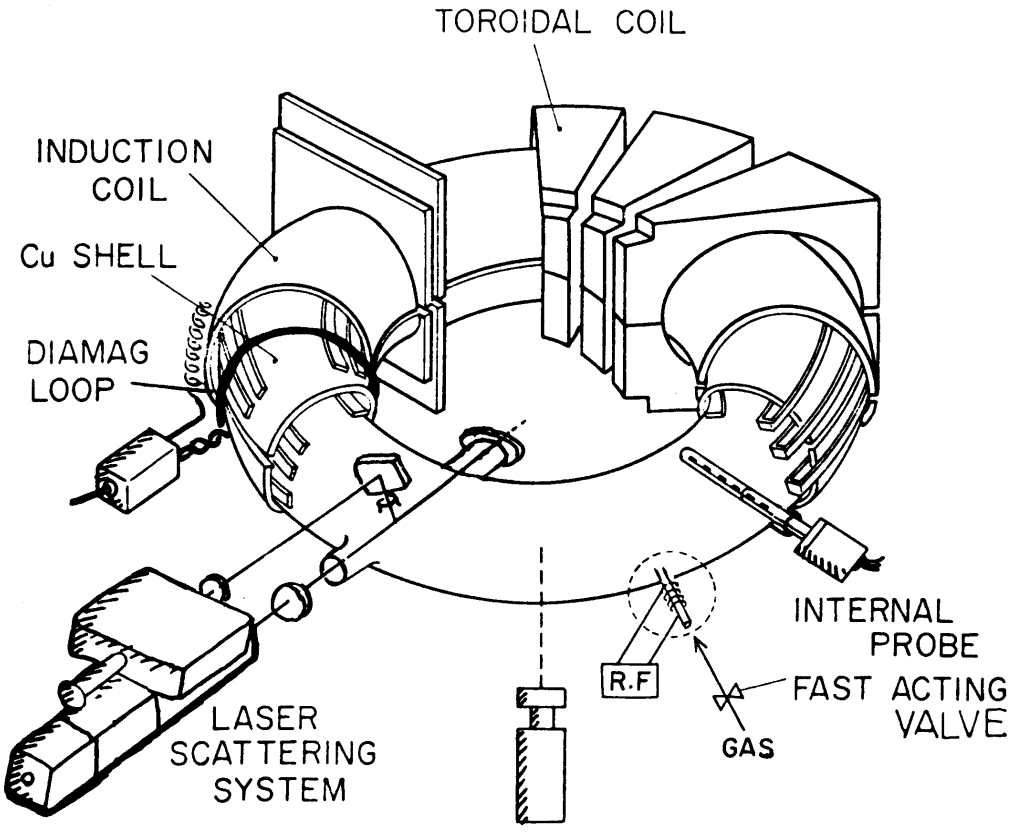
TOROIDAL COIL
INDUCTION COIL
Cu SHELL
DIAMAG LOOP
INTERNAL PROBE
R.F
FAST ACTING VALVE
GAS
LASER SCATTERING SYSTEM
STREAK CAMERA

Fig.1

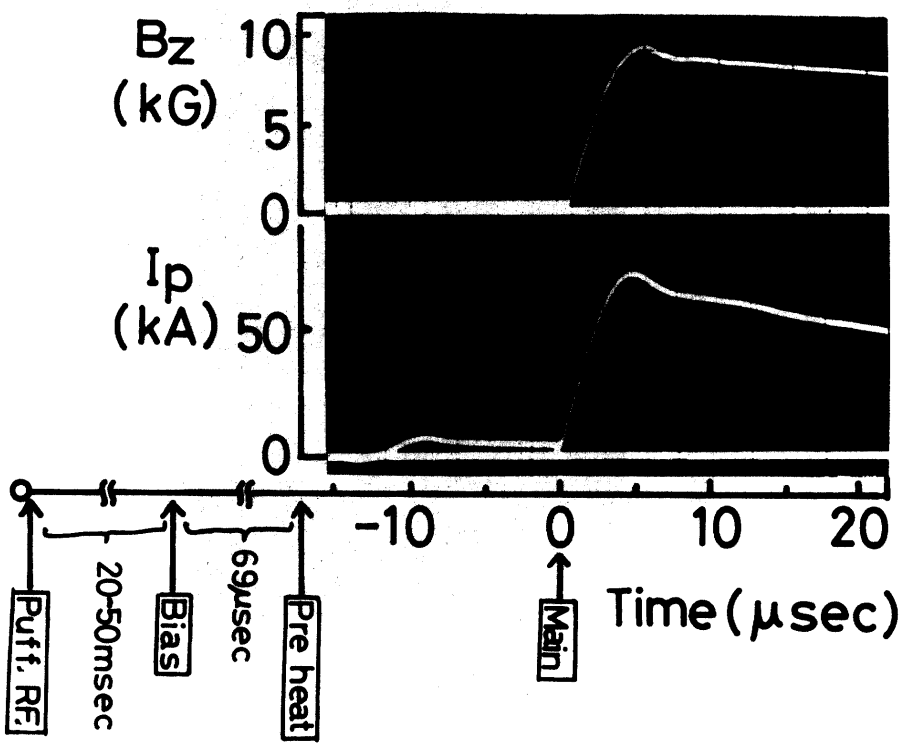
Bz
(kG)
10
5
0
Ip
(kA)
50
0
-10
0
10
20
Time (μsec)
Puff. RF
20-50msec
Bias
69μsec
Pre heat
Main

Fig.2

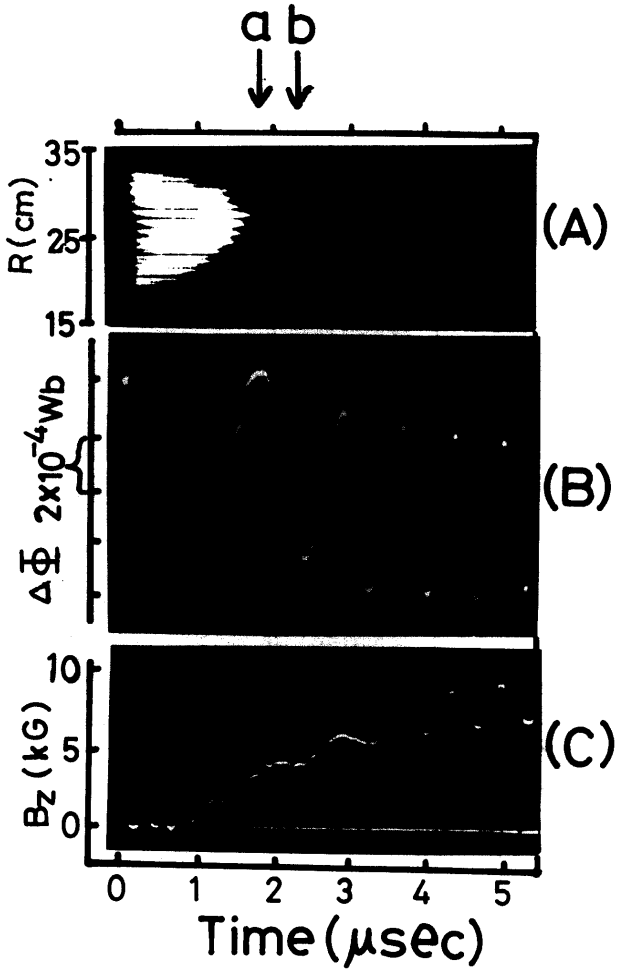

Fig.3

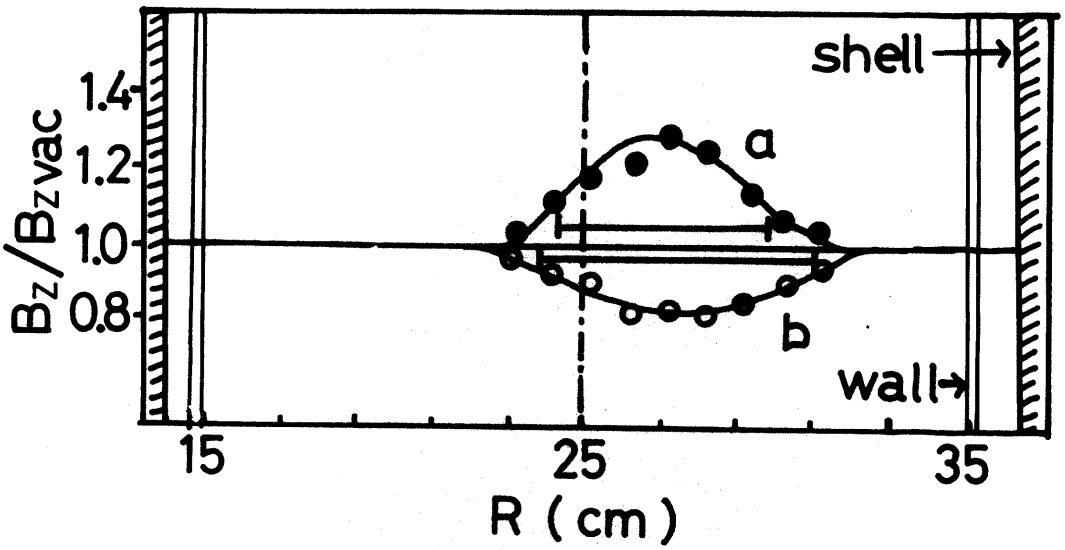

Fig.4

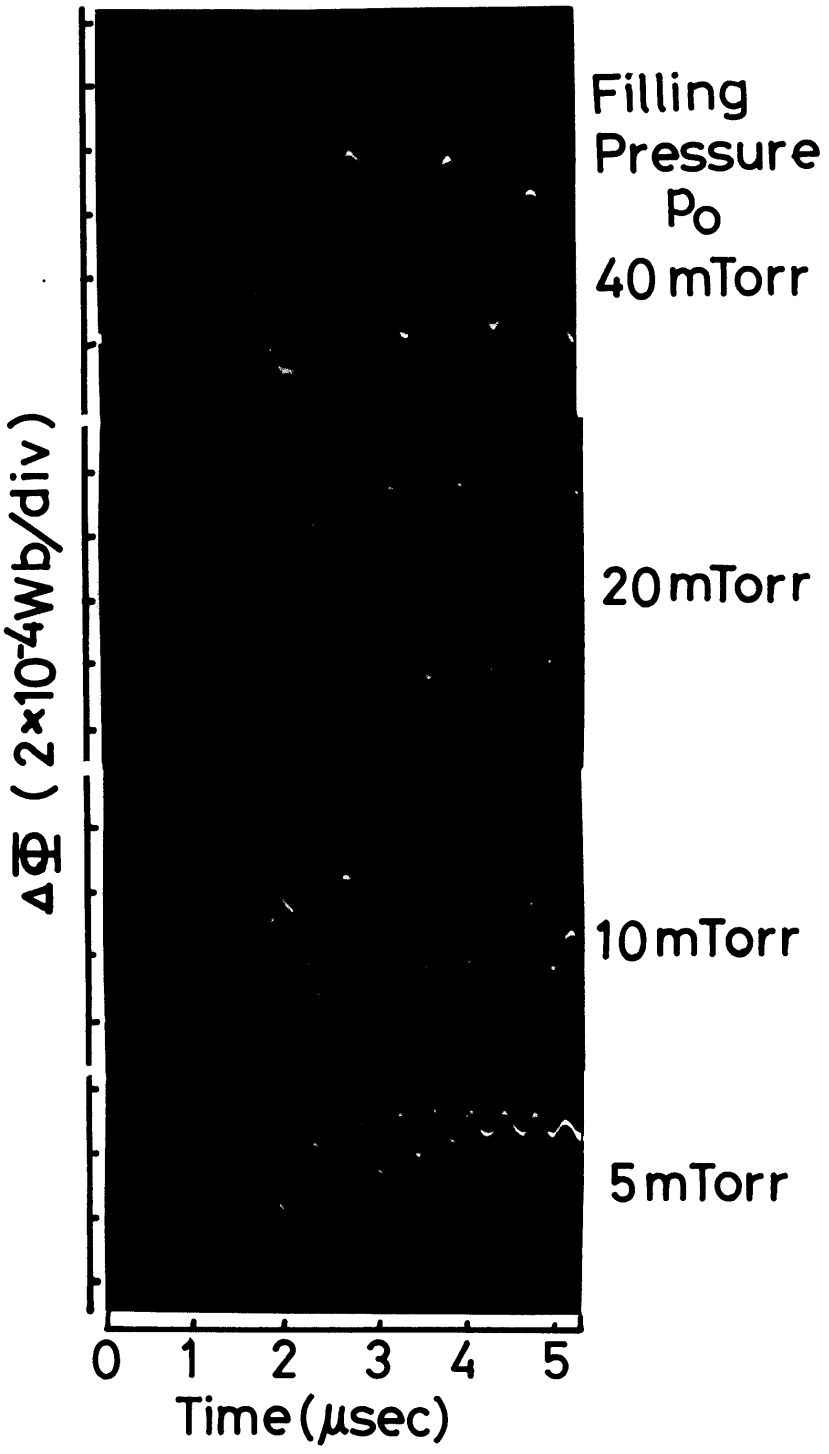
Filling
Pressure
Po
40 mTorr
20 mTorr
10 mTorr
5 mTorr
ΔΦ (2×10⁻⁴Wb/div)
0 1 2 3 4 5
Time (μsec)

Fig. 5

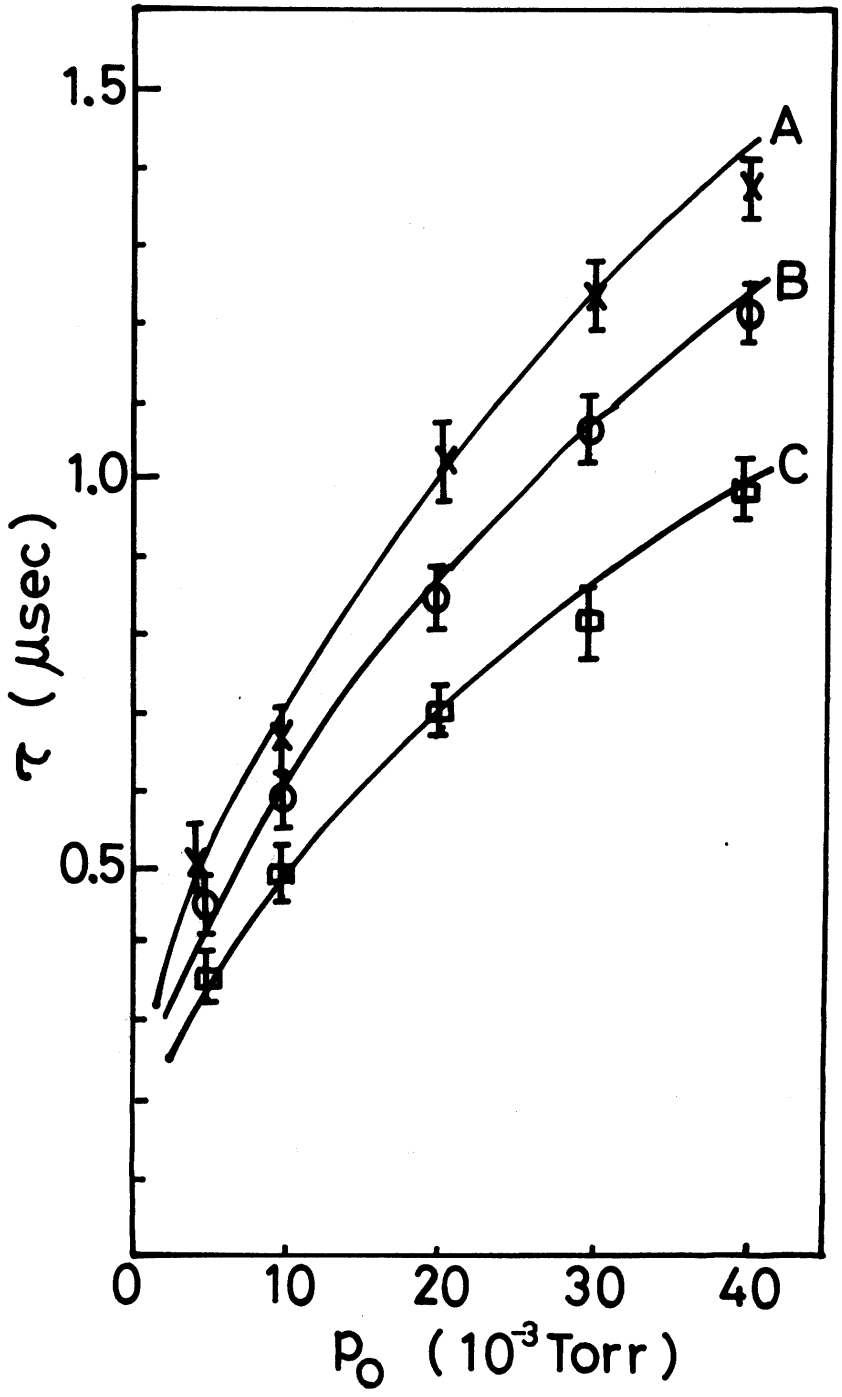

Fig.6

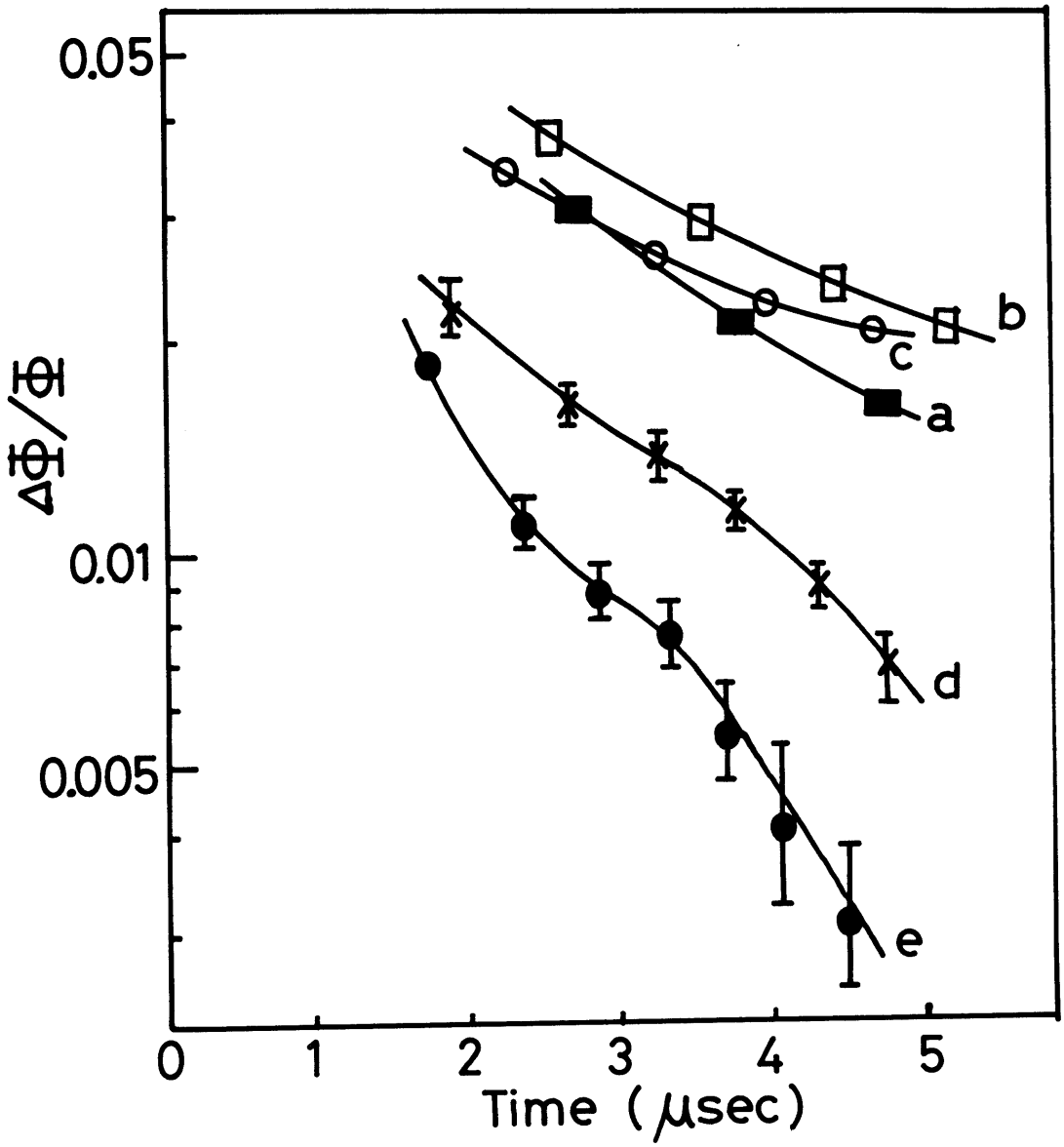

Fig.7

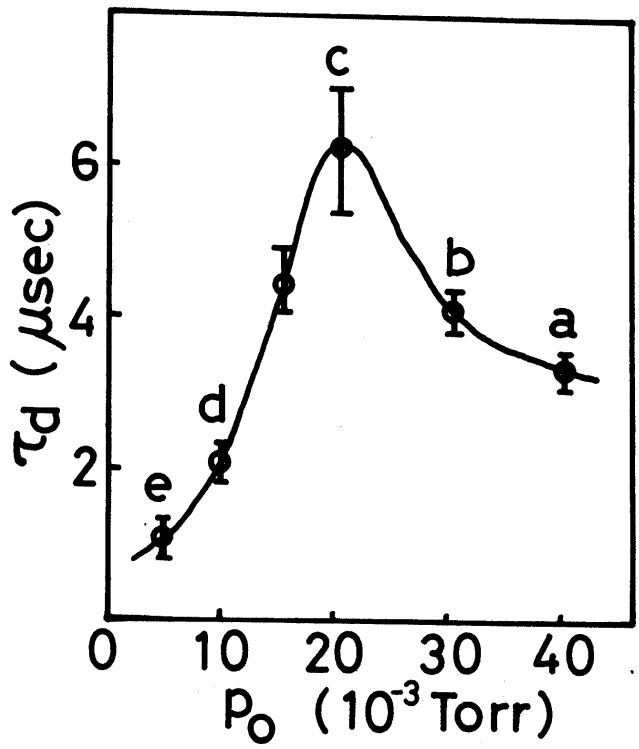

Fig.8

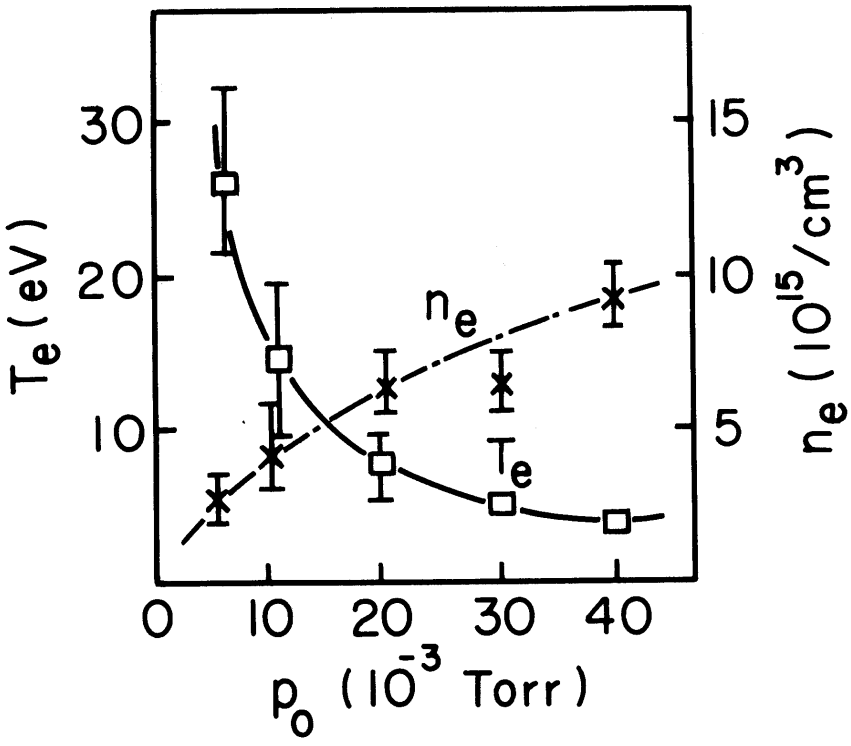

Fig.9

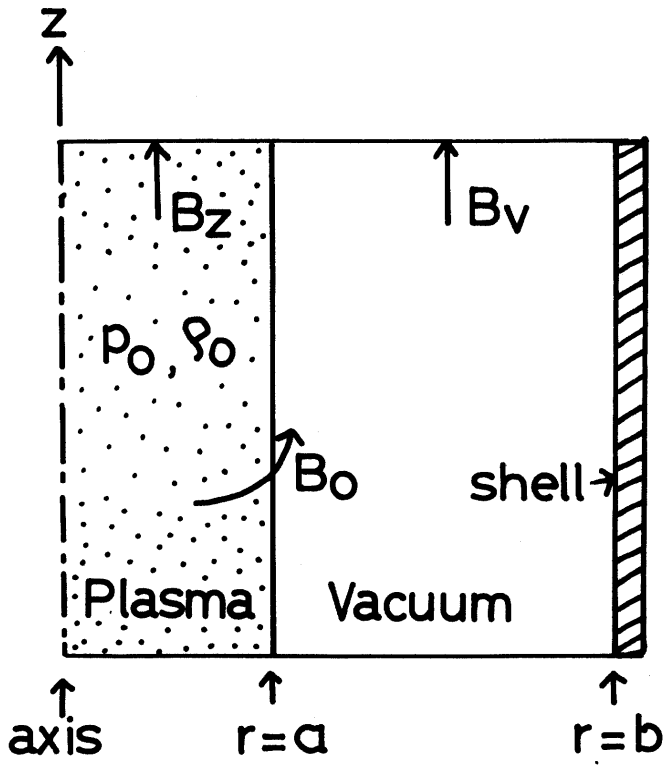

Fig.10

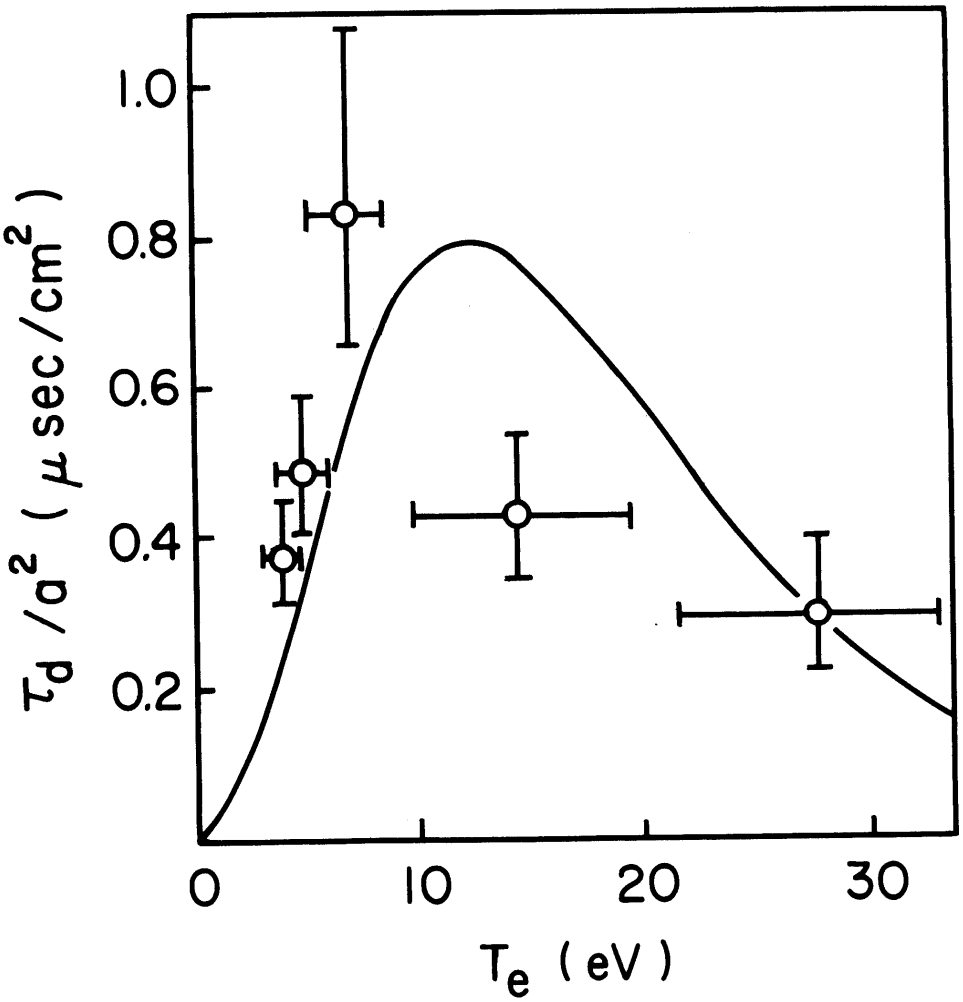

Fig.11